CONF-950713--1

SAN095-2192C

THE EFFECT OF GRAIN SHAPE ON STRENGTH VARIABILITY OF ALUMINA CERAMICS

Michael J. Readey
Senior Member, Technical Staff
Glass and Electronic Ceramics
MS 0333, Dept. 1845
Sandia National Laboratories
Albuquerque, NM 87185-0333

ABSTRACT

Fine-grained and coarse-grained aluminas containing either equiaxed or elongated grain structures were fabricated from commercial-purity and high-purity alumina powders. Compared to the high-purity aluminas, the commercial-purity aluminas having a coarse grain size and elongated grain structures exhibited significantly more pronounced flaw tolerance and T-curve behavior. T-curve behavior determined from indentation strength tests suggested that only the coarse-grained, elongated-grain alumina had a T-curve sufficient to cause stable crack extension prior to failure, a requirement for any observable improvement in reliability. In the high-purity aluminas as well as the fine-grained commercial-purity aluminas, however, it is likely that little or no stable extension occurs prior failure, suggesting that strength in these materials is dependent solely on the critical flaw size.

Strength tests on polished specimens showed the commercial-purity aluminas had a lower mean strength than the high-purity aluminas and the coarse-grained aluminas exhibited a lower mean strength compared to the fine-grained aluminas. An analysis of the mean strength versus grain size revealed that the differences in the critical flaw size alone could not account for the differences in mean strength. Instead, a combination of changes in flaw size as well as T-curve behavior were shown to be responsible for the differences in strength and flaw tolerance. T-curve behavior was also found to have a profound influence on the strength variability of alumina. For example, the Weibull modulus for the coarse-grained, commercial-purity alumina was almost twice that of the fine-grained, high-purity material. Tests with indented specimens conclusively demonstrated that improvements in reliability in these materials are not due solely to changes in the critical flaw size distribution but rather a combination of flaw size distribution and T-curve behavior.

This work was supported in part by Sandia National Laboratories, and under contract of the U.S. Department of Energy, Contract Number DE-AC04-94AL85000.

Exceptional Service in the National Interest

DISCLAIMER

Portions of this document may be illegible in electronic image products. Images are produced from the best available original document.

THE EFFECT OF GRAIN SHAPE ON STRENGTH VARIABILITY OF ALUMINA CERAMICS

Michael J. Readey
Glass and Electronic Ceramics
Sandia National Laboratories
Albuquerque, NM 87185-0333

Desiderio Kovar
Department of Materials Science and Engineering
Carnegie Mellon University
Pittsburgh, PA 15213

INTRODUCTION

During the past several years, various theories have emerged suggesting that ceramics having flaw tolerance due to an increasing fracture toughness (R or T-curve behavior) will also have an improved reliability, usually defined in terms of variability in strength.[1-3] This is an attractive approach to achieving reliable structural components, primarily because failure becomes less dependent on the size of either processing or in-service generated defects. Thus, defect-free components via expensive cleanroom processing are not required, and long-term reliability is ensured due to enhanced damage tolerance.

The link between high reliability and a rising fracture toughness is motivated by the encouraging results of transformation-toughened ceramics, namely Mg-PSZ and Ce-TZP.[2,4] In these ceramics, high Weibull moduli are typically observed in ceramics having a high fracture toughness, and low Weibull moduli are associated with zirconias having a low fracture toughness. Indeed, a systematic investigation on Mg-PSZ by Readey and McNamara demonstrated that the Weibull modulus correlates directly with enhanced T-curve behavior and flaw tolerance.[5]

However, results in monolithic, non-transforming ceramics toughened mainly by grain bridging have been less promising. For example, Kovar and Readey have shown that there is *no* improvement in reliability in spite of enhanced flaw tolerance in high-purity alumina ceramics having controlled grain sizes and equiaxed grain morphologies.[6] This same conclusion was also obtained by Rodel and co-workers on a similar material.[7]

Many systematic studies involving grain-bridging in alumina ceramics have focused on grain size as the critical microstructural feature responsible for the enhanced fracture

toughness. However, recent experimental evidence on high-purity aluminas doped with a small amount of a calcium aluminosilicate glass has suggested that grain *shape* may in fact be more important with respect to grain bridging.[8] This is not surprising; witness that elongated microstructures in silicon nitride ceramics exhibit much higher fracture toughnesses than typically achieved in silicon nitride having an equiaxed grain morphology.[9,10]

In this study, the strength variability of several aluminas having similar average grain sizes but equiaxed or elongated grain morphologies are compared and correlated to their flaw tolerance and T-curve behavior. Specifically, we address the issue of whether coarse grain microstructures having elongated grain morphologies result in greater flaw tolerance and reduced variability in strength.

EXPERIMENTAL PROCEDURE

Processing

Equiaxed microstructures were fabricated from ultra-high purity alumina powder (99.997% purity, AKP-50, Sumitomo Chemical Company). Microstructures containing elongated grains were prepared from commercial-purity alumina powder (99.7%, A-16SG, ALCOA), the predominant impurities being MgO, Na_2O, SiO_2 as well as trace quantities of CaO and FeO. Both powders were free of large agglomerates and relatively uniform in shape and size with mean particle sizes of 0.3 and 0.5 μm for the AKP-50 and A-16SG, respectively.

Powder compacts approximately 25 mm in diameter by 3 mm thick were prepared by first uniaxially pressing as-received powders in a high-purity graphite die (AF-Grade, POCO Graphite Inc.) at compaction pressures between 20 and 28 MPa. These disks were then isopressed at 280 MPa to minimize gradients in green density. The green compacts were then placed in high-purity alumina crucibles, packed in powder of the same composition, and sintered in air to 1600°C for a period of 5 hours. Some specimens were then given an additional heat-treatment at 1700°C for 25 hours in order to coarsen the microstructure. Heating and cooling rates were typically 5°C/min and 10°C/min, respectively.

Microstructure Characterization

Density measurements were conducted on all sintered aluminas using Archimedes' method with distilled water as the immersion medium. Densities were further corrected for the water temperature, and typically had an accuracy of ±0.02 g/cm^3. Quantitative information concerning the microstructure was obtained by first grinding and polishing one surface of the disks, followed by a thermal-etch treatment at 1500°C for 15 minutes to reveal the grain boundaries. Optical or scanning electron micrographs were then taken of representative areas, and the grain boundaries highlighted manually. These highlighted images were then digitized using a 300 dpi scanner, and the images converted to black and white binary images. The area of individual grains were then measured using a commercial image analysis program (Image 1.41, National Institute of Health). The two dimensional grain size (diameter) was calculated from the areas assuming spherical grains. The aspect ratio of each grain was calculated by fitting an ellipse to each grain and calculating the ratio of the major to minor axes. At least 500 grains were measured for each heat-treatment condition in order to obtain reliable statistics.

Mechanical Properties

Strength measurements were made on disk-shaped specimens using a biaxial flexure test according to ASTM standards (flat-on-3 balls).[11] Prior to testing, as-fired specimens were ground flat and polished on one side to a mirror-like finish using one micron diamond paste. The tensile surface was the polished surface in all cases. The specimens were centered on the three support balls, and loaded to failure at a rapid loading rate of 20 GPa/sec in order to minimize environmentally assisted slow crack growth. Strength was then calculated from the maximum load using thin plate theory.[11]

The indentation strength in bending (ISB) test was used to assess the flaw tolerance of the aluminas, as well to calculate the fracture toughness curves (T-curves).[12,13] Disk-shaped specimens that were polished on one side were indented with a Vickers indentor using loads 2 and 200 N. Immediately following the indentation, a drop of silicone oil was placed on the indent to exclude moisture from the indentation cracks. Specimens were then fractured as usual. After fracture, all specimens were examined using an optical or scanning electron microscope (SEM) to ensure failure originated from the indentation. Those specimens that did not fail from indentations were excluded from the analysis.

T-curves were calculated from the ISB data based on the technique of Braun *et al.*[14] Details on calibrating the indentation coefficients ψ and χ are given elsewhere.[6] The shape of the crack was determined by observing the fracture surface of indented specimens and noting the crack length and depth. Crack shape parameters for elliptical cracks were then calculated from the crack length measurements.[15]

The variability in strength was evaluated as a function of microstructure by measuring both the indented and unindented strengths of approximately 30 specimens from each material. The strength data were then ranked and each datum assigned a probability of failure according to:

$$P_f = \frac{i-0.5}{N} \qquad (1)$$

where i is ranking, and N is the total number of specimens tested. For the unindented specimens, two parameter Weibull statistics were used to determine the variability in strength, using the maximum likelihood estimator technique to calculate the Weibull modulus.[16] For the indented specimens, the flaw sizes were normally distributed, and a Gaussian distribution was used to describe the strength distribution. In this case, the strength variability was defined by the coefficient of variation by taking the ratio of the mean strength to the sample standard deviation. (In this way, the coefficient of variation is analogous to the Weibull modulus; it is a direct measure of the breadth of the strength distribution.)

RESULTS

Microstructure

Densities for all four aluminas were greater than 98 % of theoretical. Details are shown in Table 1. SEM photomicrographs of the microstructures from representative sintered specimens that were polished and thermally etched are shown in Figure 1. From the micrographs, it is evident that aluminas fired at 1600°C had a significantly finer microstructure than those heat-treated at 1700°C. In the case of the high-purity alumina, the grains are equiaxed, with a relatively narrow grain size distribution that remains

self-similar during coarsening. The commercial-purity alumina has a broader grain size distribution, with pockets of small grains surrounding larger grains. In addition, many grains are tabular or elongated in shape with one or more flat, faceted edges. Previously, it has been demonstrated in similar aluminas that flat grain boundaries and tabular grain shapes are due to the presence of a traces impurities forming a liquid phase at the grain boundaries during sintering, leading to solution-reprecipitation phenomenon that lowers the overall grain boundary energy.[17] Average grain sizes and aspect ratios are shown in Table 1. For the sake of clarification, these aluminas will be referred to as "f" (fine) or "c" (coarse) grained microstructures consisting of "eq" (equiaxed) or "el" (elongated) grain morphologies.

Indentation-Strength

Strength as a function of indentation load for the high-purity and commercial-purity aluminas are shown in Figure 2. The solid lines represent the theoretical behavior expected for materials that have a constant fracture toughness[12]; the natural strength of polished (unindented) specimens is indicated by a hatched box on the left hand side of each plot. Comparing the natural strength of the four aluminas, it is apparent that strength decreases with increasing grain size for both the commercial-purity and high-purity aluminas. Furthermore, the strength at similar mean grain sizes is lower for the commercial-purity aluminas than for the high-purity aluminas. These results are consistent with the results of previous investigations using similar aluminas.[13]

The indentation-strength response of the f-eq alumina exhibits classical brittle behavior with a slope very close to the theoretical value of -1/3, while the f-el alumina and the c-eq alumina both exhibit a slight deviation from -1/3 behavior. In contrast, the c-el alumina shows the greatest deviation from Griffith-like behavior with almost no dependence of strength on indentation load at small loads, albeit at the expense of a lower unindented strength. At large indentation loads, a plateau in the indentation-strength response is apparent in both coarse aluminas. This behavior is generally attributed to extensive lateral cracking and is not associated with flaw tolerance.[18]

Strength Variability

Weibull plots for polished (unindented) specimens are shown for the four aluminas in Figure 3. The f-eq alumina has the highest mean strength followed by the c-eq alumina, the f-el alumina, and the c-el alumina. The Weibull moduli and characteristic strengths as determined using the MLE method along with the confidence limits obtained from the parametric bootstrap technique are shown in Table 2. The Weibull moduli vary from 7.8 and 5.3 for the fine-grained and coarse-grained high-purity aluminas, respectively, to 9.2 and 14.8 for the fine-grained and coarse-grained commercial-purity aluminas. From the confidence limits, a statistical difference in Weibull modulus exists between the c-el aluminas and all of the other aluminas and also between the c-eq and the f-el alumina. Thus, only the c-el alumina, which exhibits strong flaw tolerance, shows a statistically significant higher Weibull modulus.

Strength Variability from Controlled Flaws

Strictly speaking, it is not possible to determine if the differences in strength variability observed in Figure 3 are due to flaw tolerance or whether they are instead due to a narrowing of the critical flaw distribution (*i.e.*, because of different powder sources).

Thus, strength tests were also conducted on specimens containing controlled indentation flaws at an indentation load of 100 N; the results are plotted using a probability scale in Figure 4. This indentation load was chosen because it was sufficiently large to ensure that failure always occurred from the indentation cracks and yet the extent of lateral cracking was minimized.

As expected from the indentation-strength responses of the aluminas, the f-eq alumina exhibits the lowest mean strength for indented specimens. The c-eq and f-el materials have comparable strengths which are slightly higher, while c-el alumina has the highest mean strength. The coefficient of variation, C_v, determined for each data set is not statistically different among any of the materials; it ranged from 5.7 to 6.7%. Thus, although the mean strength increases with flaw tolerance, the strength variability measured from controlled, indentation defects does not appear to be sensitive to the microstructure. These results imply that the enhanced flaw tolerance in coarse-grained aluminas does not directly lead to a reduction in the strength variability of alumina.

Crack lengths were measured in an attempt to quantify the critical flaw size distribution; a summary of the radial crack sizes is shown in Table 3 for each alumina. The f-eq had the largest flaw size and exhibited the least variability, with a coefficient of variation of 5.0%. Cracks sizes in the other materials were typically smaller, but showed an increase in variability; the coefficient of variation ranged from 8.3% to 11.7%. Thus, although controlled indentation flaws (at a constant indentation load) were used to initiate failure in all of the specimens, the critical flaw size distributions were *not* equivalent in these materials. Moreover, while the strength variability does not appear to be sensitive to the microstructure, the indentation crack lengths are clearly linked to the scale of the microstructure; variability in crack size increases with grain size and grain aspect ratio. Most significant, however, is the fact that although the variability in the indentation flaw sizes increases with grain size and aspect ratio, the strength variability is not affected by changes in the critical flaw size distribution for indented specimens.

T-Curve Behavior

The indentation-strength technique provides a relatively simple way to determine the fracture toughness at very small crack sizes comparable to the scale of the microstructure. T-curves determined from the indentation-strength method and lines corresponding to the maximum strength (i.e., tangent construction) are shown for the four aluminas in Figure 5. The T-curve for the f-eq alumina is almost flat indicating that the fracture toughness of this material is nearly constant. The f-el and c-eq aluminas have similar T-curves that rise from 3.5 MPa.m$^{1/2}$ at a crack length of 50 μm to 4.5-5 MPa.m$^{1/2}$ after 700 μm of crack extension. The c-el alumina exhibits the most pronounced T-curve rising rapidly from a toughness of 2.8 MPa.m$^{1/2}$ at 70 μm to more than 5 MPa.m$^{1/2}$ at a crack length of 700 μm.

There are a number of important features that are apparent from these T-curves; most notably, increases in T-curve behavior in alumina do not come without penalty. Consistent with previous observations in alumina and other grain-bridging ceramics, the increase in toughness at long crack lengths comes at the expense of the short-crack toughness.[19] This is particularly apparent in c-el material where the long-crack toughness is highest and the initial toughness is lowest of all of the aluminas. Another important point is that even the most pronounced T-curves rise relatively gradually in these materials. In fact, the tangency construction predicts stable crack extension from natural flaws occurs only for the c-el alumina (Fig. 5). This suggests that, with the exception of the c-el alumina, strength is dependent on the *initial* flaw size. Hence little benefit is derived from the T-curve in terms of reducing variability in strength.

DISCUSSION

Flaw Tolerance

The experimental results indicate that both grain size and grain shape play a role in determining the fracture behavior of alumina. Increasing the mean grain size only modestly increases the flaw tolerance and T-curve behavior of high-purity alumina having equiaxed grain morphologies. In contrast, the coarse-grained commercial-purity aluminas having elongated grain morphologies exhibited much stronger flaw tolerance. Such improved flaw tolerance results from a combination factors. For one, the elongated grain morphology results in a high fraction of large grains which can act as effective bridges. Second, the crack paths in the commercial-purity aluminas tended to be much more tortuous. Evidently the minor impurities present in the commercial-purity alumina powders promote intergranular fracture necessary for strong grain bridging. Thus, it appears it is the combination of weaker boundaries and large, elongated grains that are responsible for the improvement in flaw tolerance in the aluminas used in this study. For example, it was shown that neither large grains (c-eq alumina) nor an elongated grain morphology (f-el) by themselves lead to improvements in flaw tolerance. Strong flaw tolerance in the c-el alumina results due to the presence large, elongated grains and equally important, weak grain boundaries which are needed to generate a tortuous crack path necessary to get strong mechanical interlocking of the bridges.

Strength Variability

Weibull plots for polished specimens from Figure 3 indicate that, in general, strength variability decreases with increasing flaw tolerance, provided the T-curve responsible for the flaw tolerance is considerable. Similar results were found by Ting *et al.* for a series of alumina ceramics where the highest Weibull modulus was obtained for a material with a broad grain size distribution and an elongated grain shape while the poorest reliability was obtained for an equiaxed alumina with a narrow grain size distribution.[20] In addition, Hoffman and Petzow both found similar results for silicon nitride.[10] Ting *et al.* argued that the improvement in reliability in materials with increased heterogeneity in the microstructure was due a narrowing in the critical flaw size distribution. They suggested that in materials that have a narrow grain size distribution, the presence of a few large grains in only some of the specimens results in a large scatter in strength because the strength is controlled by these large grains. In contrast, materials with heterogeneous microstructures contain a more uniform dispersion of large grains and therefore, these materials exhibit less variability in strength. On the other hand, Hoffman and Petzow argued that it is T-curve behavior rather than a narrowing in the initial flaw size that is responsible for the improvement in reliability in silicon nitride ceramics.[10] Evaluating whether it is T-curve behavior or changes in the critical flaw size distribution that leads to improvements in reliability involves quantifying the critical flaw size distribution, which is experimentally difficult, particularly in coarse-grained ceramics.

Introducing controlled critical flaws through the use of indentations allows one to isolate the influence of flaw size on strength variability. In our tests, strength tests on specimens indented at an indentation load of 100 N revealed that there was essentially *no* difference in the variability in strength in aluminas with vastly different microstructures. However, measurements of the distribution in critical crack sizes, showed that distribution in the size of the cracks varied greatly depending on the material. Cracks in the coarse-grained elongated alumina had more than twice the variability compared to the fine-grained, equiaxed alumina, yet no difference in strength variability was detected. This

suggests that narrowing of the critical crack sizes distribution by itself cannot account for the improvement reliability measured in coarse-grained ceramics such as the c-el alumina in this study. This suggests that a combination of a narrow flaw population *and* strong T-curve is necessary for improved reliability in ceramics toughened by grain bridging.

CONCLUSIONS

Fine-grained and coarse-grained aluminas containing either equiaxed or elongated grain structures were fabricated from commercial-purity and high-purity alumina powders. Compared to the high-purity aluminas, the commercial-purity aluminas having a coarse grain size and elongated grain structures exhibited significantly more pronounced flaw tolerance and T-curve behavior. Thus, microstructural features other than just mean grain size were found to be important in determining the fracture properties of alumina. T-curve behavior determined from indentation strength tests suggested that only the coarse-grained, elongated-grain alumina had a T-curve sufficient to cause stable crack extension prior to failure, a requirement for any observable improvement in reliability. In the high-purity aluminas as well as the fine-grained commercial-purity aluminas, however, it is likely that little or no stable extension occurs prior failure. Thus strength in these materials is dependent solely on the critical flaw size.

Strength tests on polished specimens showed the commercial-purity aluminas had a lower mean strength than the high-purity aluminas and the coarse-grained aluminas exhibited a lower mean strength compared to the fine-grained aluminas. An analysis of the mean strength versus grain size revealed that the differences in the critical flaw size alone could not account for the differences in mean strength. Instead, a combination of changes in flaw size as well as T-curve behavior were shown to be responsible for the differences in strength and flaw tolerance. T-curve behavior was also found to have a profound influence on the strength variability of alumina. For example, the Weibull modulus for the coarse-grained, commercial-purity alumina was almost twice that of the fine-grained, high-purity material. Tests with indented specimens conclusively demonstrated that improvements in reliability in these materials are not due solely to changes in the critical flaw size distribution but rather a combination of flaw size distribution and T-curve behavior.

Acknowledgements

The authors would like to thank Stephen Bennison, Brian Lawn, Robert Cook, and Linda Braun for many helpful discussions. A critical review of this manuscript by Michael Mahoney is also greatfully appreciated. This work was supported by the U.S. Air Force Office of Scientific Research under Grant No. F4962092-J0034. Additional support was provided by Sandia National Laboratories, operated for the Department of Energy under Contract No. DE-AC04-94AL85000.

REFERENCES

1. K. Kendall, N. McN. Alford, S.R. Tan, and J.D. Birchall, The Influence of Toughness on Weibull Modulus of Ceramic Bending Strength, *J. Mater. Res.*, 1:120 (1986).
2. D.K. Shetty and J.S. Wang, Crack Stability and Strength Distribution of Ceramics that Exhibit a Rising Crack Growth Resistance (R-Curve) Behavior, *J. Am. Ceram. Soc.*, 72:1158 (1989).

3. R.F. Cook and D.R. Clarke, Fracture Stability, R-curves, and Strength Variability, *Acta metall.*, 36:555 (1992).
4. M.J. Readey, P.D. McNamara, C.L. McCallen, and B.R. Lawn, Correlations Between Flaw Tolerance and Reliability in Zirconia Ceramics, *J. Mat. Sci.*, 28:6748 (1993).
5. M.J. Readey and P.D. McNamara, R-Curve Behavior, Flaw Tolerance, and Strength Variability in Mg-PSZ, submitted to the *J. Am. Ceram. Soc.*, (1995).
6. D. Kovar and M.J. Readey, The Effect of Grain Size on Strength Variability of Alumina, *J. Am. Ceram. Soc.*, 77:1928 (1994).
7. J. Seidel, N. Claussen and J. Rodel, Reliability of Alumina Ceramics: Effect of Grain Size, *J. Europ. Ceram. Soc.*, 15:395 (1995).
8. H.L. O'Donnell, M.J. Readey and D. Kovar, Effect of Glass Additions on the Indentation Strength Behavior of Alumina, *J. Am. Ceram. Soc.*, 78:849 (1995).
9. P. Becher, Advances in the Design of Toughened Ceramics, *J. Ceram. Soc. Jap. Int. Ed.*, 99:962 (1991).
10. M.J. Hoffman and G. Petzow, Microstructural Design of Si_3N_4 Based Ceramics, *in* "Silicon Nitride Ceramics: Scientific and Technological Advances," Vol 287, Materials Research Society Proceedings, I.W. Chen, ed. MRS Publishers, Boston (1989).
11. ASTM F 394-78, Standard Test Method for Biaxial Flexure Strength (Modulus of Rupture), in Annual Book if ASTM Standards, Vol. 15.02, P.C. Fazio, ed. American Society for Testing and Materials,Philadelphia (1978).
12. B.R. Lawn, Fracture of Brittle Solids, 2nd edition. Cambridge University Press, Cambridge (1993).
13. P. Chantikul, S.J. Bennison and B.R. Lawn, "Role of Grain Size in the Strength and R-Curve Properties of Alumina, *J. Am. Ceram. Soc.*, 73:2419 (1990).
14. L.M. Braun, S.J. Bennison and B.R. Lawn, Objective Evaluation of Short Crack Toughness Curves Using Indentation Flaws: Case Study on Alumina-Based Ceramics, *J. Am. Ceram. Soc.*, 64:533 (1981).
15. P.C. Paris and G.C.M. Sih, Stress Analysis of Cracks, in Fracture Toughness Testing and its Applications. American Society for Testing and Materials, Philadelphia (1965).
16. C.A. Johnson and W.T. Tucker, Weibull Estimators for Pooled Fracture Data, *in* "Life Prediction Methodologies and Data for Ceramic Materials", C.R. Brinkman and S.F. Duffy, eds. American Society for Testing and Materials, Philadelphia (1994).
17. W.A. Kaysser, M. Sprissler, C.A. Handweker, and J.E. Blendell, Effect of a Liquid Phase on the Morphology of Grain Growth in Alumina, *J. Am. Ceram. Soc.*, 70:339 (1987).
18. R.F. Cook, E.G. Liniger, R.W. Steinbrech, and F. Deueler, Sigmoidal Indentation-Strength Characteristics of Polycrystalline Alumina, *J. Am. Ceram. Soc.*, 77:303 (1994).
19. N.P. Padture, J.L. Runyan, S.J. Bennison, L.M. Braun, and B.R. Lawn, Model for Toughness Curves in Two-Phase Ceramics, *J. Am. Ceram. Soc.*, 76:2241 (1993).
20. J.M. Ting, R.Y. Lin and Y.H. Ko, Effect of Powder Characteristics on Microstructure and Strength Characteristics of Sintered Alumina, *Am. Ceram. Soc. Bull.*, 70:1167 (1991).

Table 1. Physical properties of alumina ceramics.

Alumina	Heat-Treatment	Density (g/cm^3)	Grain Size (μm)	Aspect Ratio
High-Purity*	1600°C/5h	3.91	5.0 ± 2.6	1.5
High-Purity*	1600°C/5h + 1700°C/25h	3.93	10.2 ± 4.9	1.5
Commercial-Purity**	1600°C/5h	3.93	4.0 ± 3.9	2.1
Commercial-Purity**	1600°C/5h + 1700°C/25h	3.91	12.8 ± 11.4	2

* AKP-50, 99.997% purity, Sumitomo Chemical Company.
**A16-SG, 99.7% purity, ALCOA

Table 2. Characteristic strengths, Weibull moduli including 90% confidence limits (m_5 and m_{95}) for the four aluminas. Note that only the c-el shows any statistically significant reduction in strength variability.

Alumina	σ_o (MPa)	m	m_5	m_{95}
f-eq	507	7.8	6.1	10.5
c-eq	369	5.3	4.2	7.1
f-el	346	9.2	7.4	11.9
c-el	243	14.8	12.1	19.8

Table 3. A comparison of the indentation crack lengths generated from a 100 N Vickers indentation. Note that the f-eq alumina exhibits significantly less variability in crack length relative to the other aluminas.

Alumina	Crack Length (μm)	Coefficient of Variation (%)
f-eq	221 ± 11	5
c-eq	182 ± 21	11.7
f-el	181 ± 15	8.3
c-el	192 ± 22	11.6

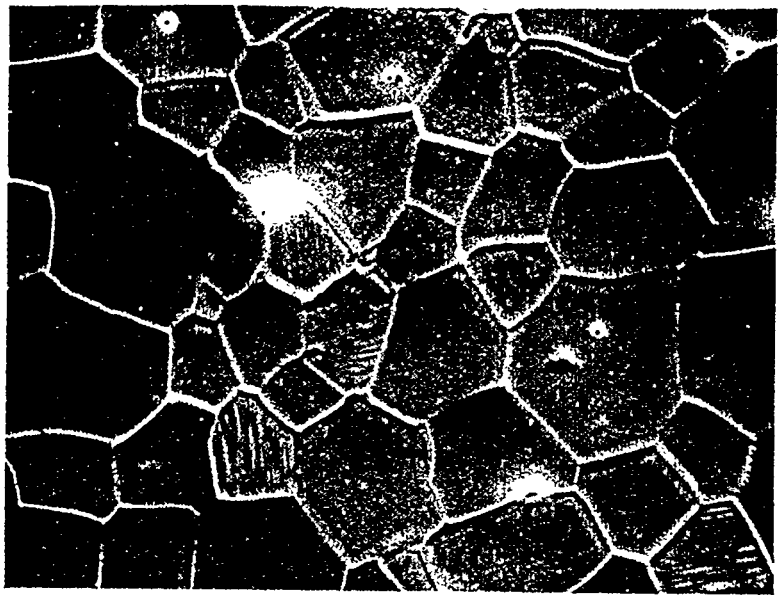

(a)

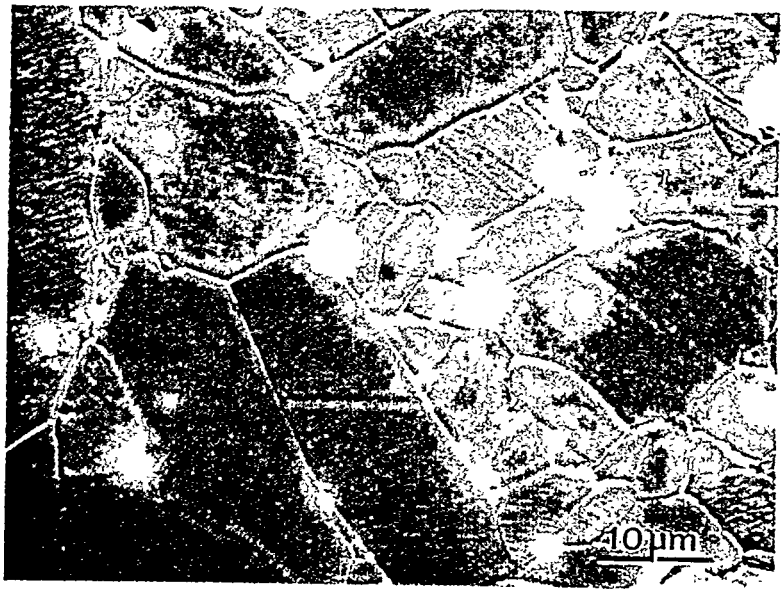

(b)

Figure 1. SEM micrographs showing the (a) high-purity alumina (b) commercial-purity aluminas sintered at 1600°C/5h.

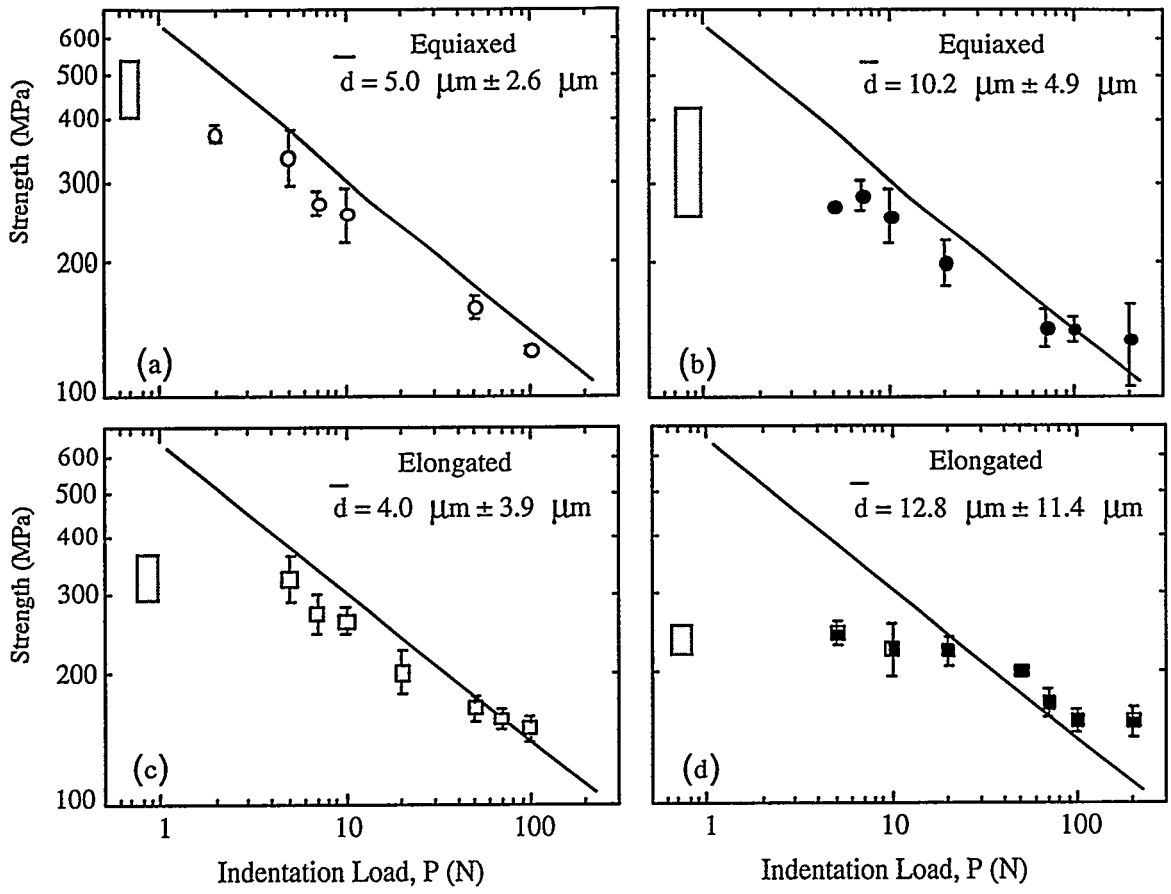

Figure 2. Strength as a function of indentation load (log-log scale) for the f-eq (a), c-eq (b), f-el (c), and c-el (d) alumina. See text for details.

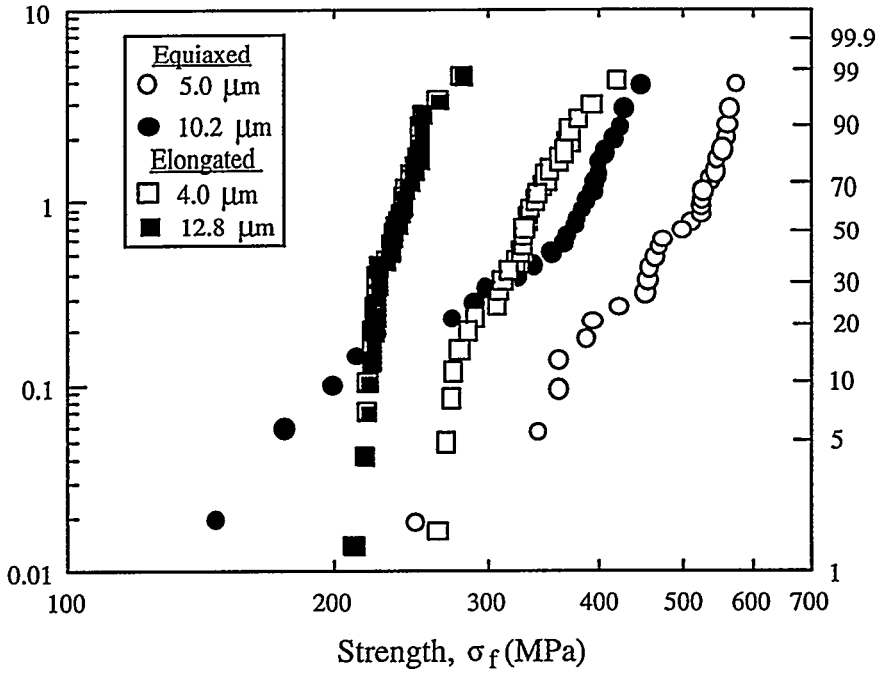

Figure 3. Weibull plot for polished specimens for the four aluminas. Although the high-purity, equiaxed aluminas have a higher average strength, the commercial-purity, elongated microstructure show the higher reliability.

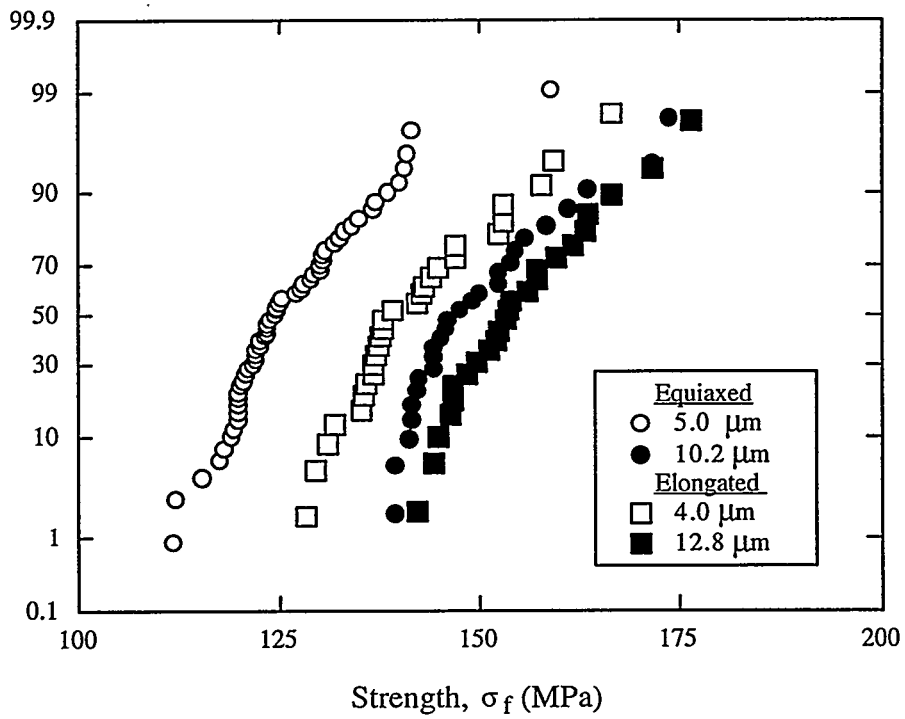

Figure 4. Strength variability for specimens that failed from 100 N Vickers indentations plotted using a probability scale. The fine-grain aluminas have a lower mean strength but the variability in strength is similar in all of the materials.

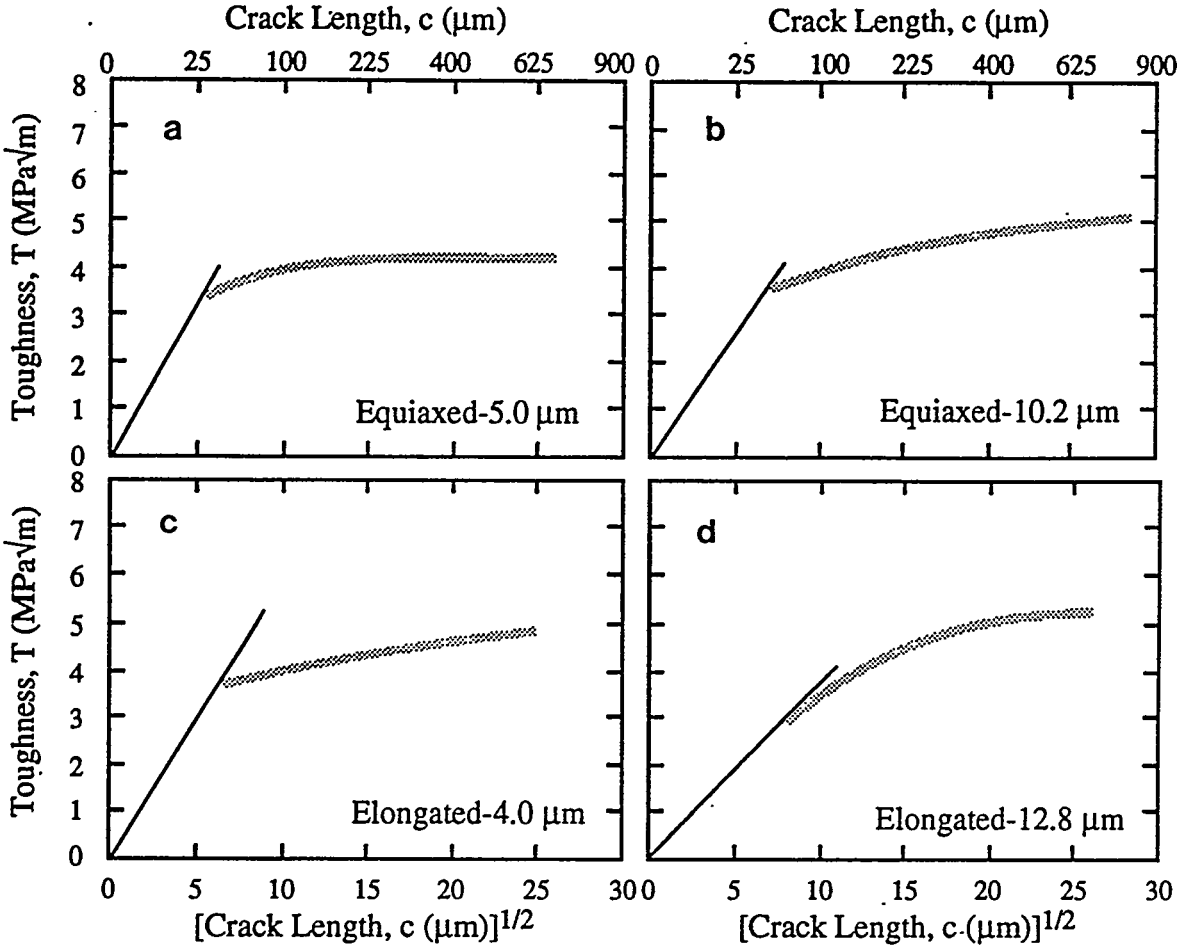

Figure 5. Toughness curves calculated from the indentation-strength data. Only the c-el alumina (d) exhibits pronounced T-curve behavior.

M96000671	DOEOR21400T490	559	4470
M96000672	DOEOR21400T491	559	4468
M96000673	DOEOR21400T492	559	4468
M96000674	DOEOR21400T493	559	4468
M96000675	DOEOR21400T494	559	4468
M96000676	DOEOR21400T495	559	4468
M96000677	DOEOR21400T496	559	4468
M96000678	DOEOR21400T497	559	4468
M96000679	DOEOR21400T498	559	4468
M96000681	DOECE503433	559	4470
M96000682	UCRLJC121119	559	4468
M96000683	DOERL9543	559	4468
M96000684	SAND952062C	559	4468
M96000685	SAND952245C	559	4468
M96000686	ORNLM1676	559	4468
M96000687	DOEOR21400T499	559	4468
M96000688	BNL52481	559	4468
M96000689	WRB9508	559	4468
M96000690	DOECE15554T5	559	4468
M96000691	DOEAL62350133REV1VER6	559	4468
M96000692	SAND942217	559	4468
M96000693	PNL10791	559	4468
M96000695	NUREGCP0148	559	4468
M96000696	DOEEIA0598	559	4468
M96000697	UCRLJC121589	559	4468
M96000698	SAND952192C	559	4468
M96000699	SAND940244	559	4468
M96000700	SAND951950	559	4468